

Positron emission tomography

A.M.J. Paans

Department of Nuclear Medicine & Molecular Imaging, University Medical Center Groningen, The Netherlands

Abstract

Positron Emission Tomography (PET) is a method for measuring biochemical and physiological processes *in vivo* in a quantitative way by using radiopharmaceuticals labelled with positron emitting radionuclides such as ^{11}C , ^{13}N , ^{15}O and ^{18}F and by measuring the annihilation radiation using a coincidence technique. This includes also the measurement of the pharmacokinetics of labelled drugs and the measurement of the effects of drugs on metabolism. Also deviations of normal metabolism can be measured and insight into biological processes responsible for diseases can be obtained. At present the combined PET/CT scanner is the most frequently used scanner for whole-body scanning in the field of oncology.

1 Introduction

The idea of *in vivo* measurement of biological and/or biochemical processes was already envisaged in the 1930s when the first artificially produced radionuclides of the biological important elements carbon, nitrogen and oxygen, which decay under emission of externally detectable radiation, were discovered with help of the then recently developed cyclotron. These radionuclides decay by pure positron emission and the annihilation of positron and electron results in two 511 keV γ -quanta under a relative angle of 180° which are measured in coincidence. This idea of Positron Emission Tomography (PET) could only be realized when the inorganic scintillation detectors for the detection of γ -radiation, the electronics for coincidence measurements, and the computer capacity for data acquisition and image reconstruction became available. For this reason the technical development of PET as a functional *in vivo* imaging discipline started approximately 30 years ago.

PET employs mainly short-lived positron emitting radiopharmaceuticals. The most widely used radionuclides are: ^{11}C ($t_{1/2} = 20$ min), ^{13}N ($t_{1/2} = 10$ min), ^{15}O ($t_{1/2} = 2$ min) and ^{18}F ($t_{1/2} = 110$ min). Carbon, oxygen, nitrogen and hydrogen are the elements of life and the building blocks of nearly every molecule of biological importance. However, hydrogen has no radioactive isotope decaying with emission of radiation which can be detected outside the human body. For this reason, a fluorine isotope is often used to replace a hydrogen atom in a molecule. Due to these short half-lives the radionuclides have to be produced in house, preferably with a small, dedicated cyclotron. Since the chemical form of accelerator-produced radionuclides can only be simple, input from organic- and radiochemistry is essential for synthesis of the desired complex molecules. Input from pharmacy is required for the final formulation and pharmacokinetic studies and are also required for (clinical) application. Longer lived positron emitting radionuclides such as ^{52}Fe , ^{55}Co , ^{64}Cu , ^{75}Br , ^{76}Br , ^{124}I are sometimes commercially available or obtainable from research facilities with larger accelerators. Also a few generator systems do exist: the $^{68}\text{Ga}/^{68}\text{Ge}$ and the $^{82}\text{Rb}/^{82}\text{Sr}$ generator. ^{68}Ga and ^{82}Rb have half-lives of 68 m and 75 s respectively.

At the moment small dedicated cyclotrons are a commercially available product. These accelerators are one- or two-particle machines with fixed energies. At the moment mostly negative-ion machines are being installed because of their relatively simple extraction system and high extraction efficiency. They are installed complete with the targetry for making the four above-mentioned short-

lived radionuclides in batches up to 100 GBq or even more. Also the chemistry for some simple chemical products is incorporated, e.g., $^{11}\text{CO}_2$, ^{11}CO , C^{15}O , C^{15}O_2 , H_2^{15}O etc. Sometimes synthesis modules for the preparation of more complex molecules, e.g., ^{18}FDG , $^{18}\text{F-DOPA}$, ^{18}FLT , H^{11}CN , $^{11}\text{CH}_4$, $^{11}\text{CH}_3\text{I}$ or $^{13}\text{NH}_3$ are also available from the cyclotron manufacturer or a separate specialized company. These products become available via dedicated, automated systems or via a programmable robotic system. Other radiopharmaceuticals have to be set up individually in each PET centre.



Fig. 1: Scanditronix MC-17F cyclotron as installed in 1991 in the UMCG for the production of ^{11}C , ^{13}N , ^{15}O and ^{18}F . Beams available are 17 MeV protons or 8.5 MeV deuterons. Targets are mounted at the target ladder at the beam exit of the cyclotron MC-17.

The state-of-the-art positron camera is a complex radiation-detection technology product combined with a relative large computing power for data acquisition and image reconstruction. The basic detector in a modern PET camera is scintillator as a detector block divided in e.g. 8×8 subdetectors or pixelated larger size crystals and read out by photomultiplier tubes (PMTs). By adding and subtracting the individual signals of the PMTs the scintillating subdetectors can be identified. Around 70 blocks will form a ring and 4 of these rings can be added to get an axial field of view of approximately 15–16 cm. In this way 31–63 or even more planes are imaged simultaneously with a spatial resolution of 4–7 mm FWHM depending on the specific design of the tomograph. The septa between the adjacent subdetector rings can also be retracted creating a much higher sensitivity in this 3D mode at the cost of a larger scatter fraction. Hardware and software for data acquisition, image reconstruction and for image manipulation are available. Positron cameras can measure the radioactivity in absolute terms, Bq/pixel, which is an unique feature. This is possible because the coincidence technique allows for the correction of the attenuation of radiation inside the body of the individual patient. This correction is accomplished by making an individual ‘transmission image’ with an external positron emitting source. This individual transmission image can also be used to correct for scattered radiation which is present in the image after a 3D-acquisition. This external source is built into the camera and can be extended from its well shielded storage box. At the moment the attenuation map is also available using single photon emitters or even a CT image. To translate the measured radioactivity distribution into functional or physiological parameters, compartment models

have been developed for radiopharmaceuticals with known metabolite profiles. Although only a few measurable quantities, i.e., tissue and plasma concentration (the latter by taking blood samples) are available, it is still possible to calculate, for example, the glucose consumption by employing a dynamic data acquisition protocol in combination with a compartment model. It is also possible to make a whole-body scan by moving the patient step-wise through the PET camera. By projection of the transverse section images, a whole-body overview can be made.

The most recent development is the physical combination of PET and a CT into a PET/CT unit. Next to the obvious easier way of coregistration of the individual images, the CT is also used for the attenuation correction of the PET images. By segmentation of the CT images and then inserting the correct attenuation coefficients for 511 keV at the different tissues a correct attenuation map is obtained. In fact it is the most popular version of PET-scanning at the moment and in use as whole body dual mode scan it is the most widely used scan mode especially in the field of oncology.

A PET centre is the combined relevant knowledge of chemistry, medicine, pharmacy and physics and it should be staffed by all these disciplines in a good co-operating team.

2 Accelerators for PET radionuclide production

In the energy range from 10–20 MeV, all four basic radionuclides ^{11}C , ^{13}N , ^{15}O and ^{18}F can be produced. In general, the device of choice is a cyclotron, not a linear accelerator, because in this energy range the cyclotron is a versatile and economic solution. Although at higher energies a larger part of the excitation function can be exploited resulting in a higher yield, some companies on purpose designed cyclotrons at the low energy range of 10–11 MeV protons for economical reasons.

Radionuclides can be produced by using neutrons or charged particles as irradiation source. Irradiation by neutrons leads to neutron capture and so to neutron-rich nuclides. The use of charged particles like protons or deuterons leads to nuclear reactions of the type (p,xn) or (p,α) which results in the production of neutron-deficient nuclides, see Table 1. Both types of nuclear reactions lead to radioactive nuclei. Accelerators and nuclear reactors are complementary production units [1–3].

Table 1: Nuclear reactions in use for the most common radionuclides in PET

Nuclear reaction	Q-value	Target	Product
$^{14}\text{N}(p,\alpha)^{11}\text{C}$	– 2.9 MeV	$\text{N}_2 (+\text{O}_2)$	$^{11}\text{CO}_2$
$^{6}\text{O}(p,\alpha)^{13}\text{N}$	– 5.2 MeV	$^6\text{H}_2\text{O}$ + EtOH	$^{13}\text{NO}_3$, $^{13}\text{NO}_2$ $^{13}\text{NH}_3$
$^{14}\text{N}(d,n)^{15}\text{O}$	+ 5.1 MeV	$\text{N}_2 (+\text{O}_2)$	$^{15}\text{O}_2$
$^{15}\text{N}(p,n)^{15}\text{O}$	– 3.5 MeV	$^{15}\text{N}_2 (+\text{O}_2)$	$^{15}\text{O}_2$
$^{18}\text{O}(p,n)^{18}\text{F}$	– 2.4 MeV	H_2^{18}O $^{18}\text{O}_2 (+\text{F}_2)$	$^{18}\text{F}^-$ $^{18}\text{F}_2$
$^{20}\text{Ne}(d,\alpha)^{18}\text{F}$	+ 2.8 MeV	Ne (+ F_2)	$^{18}\text{F}_2$

The targets are most often installed just outside the cyclotron. Sometimes a short beam line is installed to focus the beam on the target. The big advantage of the acceleration of negative ions is that after passing through a carbon stripper foil, all electrons are removed and the now positive charged beam is automatically bent out of the machine. An extraction efficiency of 100% is possible and by positioning the stripper foil only half way in the beam, multiple (at least 2) extracted beams are also possible.

The transport of the irradiated material can be very easy in the case of a gas target. Just a normal flow can carry the radioactivity over rather long distances. In case of a fluid target, a helium flow through thin tubing can push the irradiated material into the desired position. With solid targets an exchange system or train system can transport the target or target material. The local situation will dictate which particular solution is selected.

Due to the nature of the induced nuclear reaction (p,xn) there is a change in element:



The term 'carrier free' is used when no 'cold' material of the same chemical composition as the radioactive species is present. This is very difficult to achieve because often a natural dilution occurs. Often the term 'non carrier added' or 'nca' production is used. This means no cold material of the same chemical identity is added on purpose by the investigator during preparation of the radiopharmaceutical.

Specific activity is the amount of radioactivity per gram or mole. The theoretical maximum of the specific activity is related to the number of radionuclides through: $A \text{ (Bq)} = N_0 \lambda$ with $\lambda = \ln 2/t_{1/2}$ the decay constant. The maximal specific activities for a few radionuclides are given in Table 2.

Table 2: The maximum, theoretical specific activity for the four most important PET radionuclides

Radionuclide	Specific activity
^{11}C	$9.2 * 10^9 \text{ Ci/mol} = 340 \text{ TBq}/\mu\text{mol}$
^{13}N	$1.9 * 10^{10} \text{ Ci/mol} = 680 \text{ TBq}/\mu\text{mol}$
^{15}O	$9.2 * 10^{10} \text{ Ci/mol} = 3400 \text{ TBq}/\mu\text{mol}$
^{18}F	$1.7 * 10^9 \text{ Ci/mol} = 63 \text{ TBq}/\mu\text{mol}$
^{14}C	$6.2 * 10^1 \text{ Ci/mol} = 2.3 \text{ MBq}/\mu\text{mol}$

The maximum theoretical specific activity is determined by the half-life. This difference in half-life for ^{11}C and ^{14}C (20.4 min 5730 yr) explains the big difference in specific activity. In reality, these theoretical maxima in specific activity are never reached. Very special precautions have to be taken to keep the dilution factor low. With a carrier-free or non-carrier-added synthesis one expects no toxic effects (e.g., H^{11}CN or C^{15}O are not toxic on this level) and no physiological or pharmacological effects (tracer principle) are expected.

The most commonly used reactions are

$^{14}\text{N}(p,\alpha)^{11}\text{C}$ with nitrogen with a little (2%) oxygen mixed in as target material. The radioactive product is $^{11}\text{CO}_2$. Dilution can easily occur with CO_2 from the atmosphere.

$^{14}\text{N}(p,\alpha)^{13}\text{N}$ with H_2O as target material. After irradiation the ^{13}N is available as nitrate or nitrite in the water. Distillation under steam with Devarda's alloy yields $^{13}\text{NH}_3$. Nowadays, by addition of ethanol into the target water, in-target production of ^{13}N -ammonia is also possible.

$^{14}\text{N}(d,n)^{15}\text{O}$ with nitrogen with a little oxygen (<5%) mixed in as target material. The most common use of oxygen-15 is for rCBF (regional cerebral blood flow) studies. Oxygen-15 labelled water can be produced in two ways: i) convert according to $^{15}\text{O}_2 + \text{C} \text{ (400}^\circ\text{C)} \rightarrow \text{C}^{15}\text{O}_2$. Upon inhalation, the C^{15}O_2 is instantaneously converted into H_2^{15}O in the lung via a reaction catalysed by the enzyme carbonic anhydrase. It is also possible to convert the oxygen into water according to: $^{15}\text{O}_2 + 2\text{H}_2 \rightarrow 2\text{H}_2^{15}\text{O}$ in an oven with Pt catalyt. This yields a continuous stream of H_2^{15}O which can be administered intravenously.

The most common way to produce ^{18}F is the $^{18}\text{O}(\text{p},\text{n})^{18}\text{F}$ reaction with H_2^{18}O as target material. Oxygen-18 enriched water (>90%, costs in April 2005: €90.00 /g). The ^{18}F is available as F^- ion in the water. After separation of the fluoride and the water the fluoride is available for chemistry. The water can be used again after distillation to eliminate impurities. The enrichment grade will of course be diminished by the distillation procedure. The specific activity of the fluorinated end-product can easily be better than that of carbon-11 product because fluor is less abundant than CO_2 , for example, so less tracer dilution will occur.

A second method for the production of ^{18}F is by the $^{20}\text{Ne}(\text{d},\alpha)^{18}\text{F}$ reaction. To the Ne-gas F_2 is added to coat the target chamber wall. If this coating is not done, all the produced ^{18}F is adsorbed by the wall and can not be extracted for further chemistry. The ^{18}F becomes available as F_2 and the relative low specific activity depends on the amount of fluorine which is added before irradiation. The two different chemical forms of ^{18}F allow different chemical labelling strategies.

3 PET scanner

There are two decay possibilities for neutron deficient radionuclides: positron emission or electron capture (EC):

- Positron decay $\text{p} \rightarrow \text{n} + \beta^+ + \nu$
- Electron capture $\text{p} + \text{e}^- \rightarrow \text{n} + \nu$

Positron decay is only possible if an energy of $2m_0c^2$ (= 1022 keV) or more is available, otherwise Electron Capture (EC) will occur. In practice a surplus in energy is required before a large percentage of the decay occurs by positron decay channel instead of EC. The neutrino (ν) is a particle with zero rest mass which shares its kinetic energy with the positron or the neutron.

With positron decay two conservation laws have to be obeyed:

- i) conservation of energy and
- ii) conservation of momentum.

The positron is slowed down in the tissue by collisions: at the end of track a positronium, a hydrogen like atom, is formed by the positron and an electron. The positron and electron are anti-particles and so they will annihilate. In the annihilation process, two gamma-quanta of 511 keV back-to-back or co-linear are generated. In this way both conservation laws are obeyed. A three-quanta annihilation is also possible within the two conservation laws. The three-quanta annihilation only happens if the formed positronium is in its triplet state, which is rare, with a half-life of 7 μs . In the singlet state the positronium decays with a lifetime of 8 ns [4].

To image the annihilation radiation one should profit from its unique properties: 511 keV co-linear (180°) and simultaneously [5–9]. So coincidence measurements and ideally measurement of the time difference, so-called Time Of Flight (TOF) measurement, should be done. For two detectors, A and B, at a distance $2d$ and a point source P at distance x from the centre line the difference in distance is:

$$\text{PA} - \text{PB} = (d + x) - (d - x) = 2x$$

time involved:

$$\Delta t = 2x/c \quad \text{with } 2x = 1 \text{ mm}, \quad \Delta t = 3.3 \text{ ps.}$$

Scintillation detectors with these timing properties and high sensitivity for 511 keV radiation do not exist at the moment. Until approximately 1983, mostly NaI detectors systems have been used. Since then BGO (Bismuthgermanate: $\text{Bi}_4\text{Ge}_3\text{O}_{12}$) material in a block-detector structure is mainly being used. The use of BGO rather than NaI resulted in improved efficiency because of the higher density and Z-value of this material. Originally the detector with its single PMT determined the spatial resolution. To improve also in spatial resolution, a gamma camera read-out with four PMTs was designed on a single BGO crystal. Due to the thickness of the BGO detector the scintillation light spread out quite a bit. By cutting the BGO detector into 8×8 sub-detectors a light guiding was constructed which allowed, together with the four PMTs, a spatial resolution basically the same as the size of the sub-detectors, Figs. 2 and 3. The drawback of BGO, see also Table 3, is its relatively low light output (15% of the output of NaI). Recently GSO (Gadolinium-ortho-silicate: Gd_2SiO_5), a scintillator which has been used as a single crystal, has come into use, as a pixelated area detector with a gamma camera logic read-out. The advantage of GSO is its better light output (25% of the output of NaI) than BGO. LSO (Lutetium-ortho-silicate: Lu_2SiO_5), one of the most recently discovered scintillators, has been tested for application in PET scanners. The relatively high light output (75% of the output of NaI) is a big advantage and the short decay time warrants a high maximum count rate. The disadvantage of a natural radioactive component in natural Lu has no consequences as long as coincidence measurements are performed. At the moment (April 2005) General Electric PET scanners use BGO, Philips PET scanners use GSO, and Siemens PET scanners use LSO as detector material.

Table 3: Properties of the different detector materials

Detector material	NaI	BGO	GSO	LSO
Density (g/cm^3)	3.67	7.13	6.7	7.4
Eff At number	51	75	59	66
Hygroscopic	y	n	n	n
Decay time (ns)	230	300	56/600	40
Rel light yield	100	15	25	75
Energy resolution ^{*)}	7.8%	10.1%	9.5%	10%

^{*)} NB: These numbers are for a single crystal with PMT.

There are different types of PET scans, the scans which can be routinely performed are

- Static scan: a set of transverse section images. Interpretation by visual inspection and/or by left/right differences. Often sufficient for a clinical study.
- Dynamic scan: a set of consecutive scans in time. The distribution as a function of time can be studied in the field of view. Information as a function of time is an essential input for the derivation of functional parameters. Also arterial blood sampling, establishing the so-called ‘input function’, and metabolite analysis are often required for quantitation of a functional parameter.
- Whole-body (WB) scan: a set of consecutive scans covering the whole body. By combining these scans in a 3-dimensional volume, an overview of radioactivity in the body is visualized. A whole-body scan is often used in oncological studies, e.g., to detect metastases or unknown primary tumors. Nowadays most WB scans are performed using a combined PET/CT scanner, see Fig. 4.

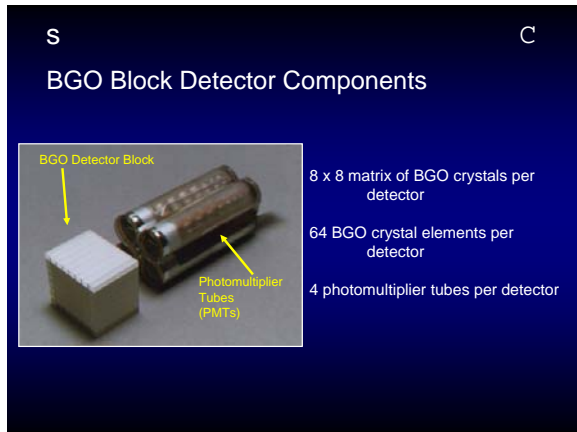


Fig. 2: BGO block detector with PMTs (Courtesy Siemens)

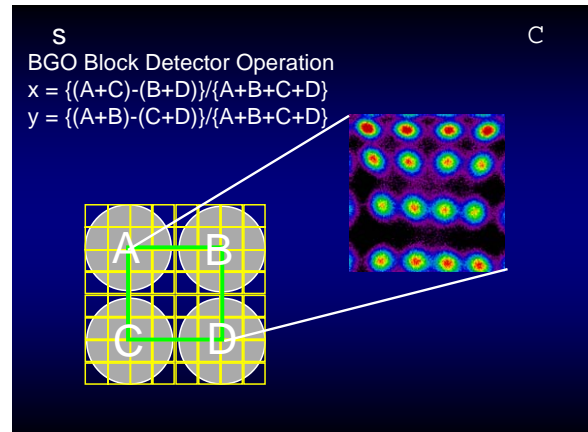


Fig. 3: Spatial resolution of a BGO block detector with 4 PMTs. The position resolution of the 4 x 4 crystals in the green central square are displayed on the right side. Position is calculated according to the outputs of PMTs A, B, C and D. (Courtesy Siemens)



Fig. 4: The Siemens Biograph, a combined PET/CT scanner (Courtesy Siemens)

In order to limit scattered radiation from the object reaching the detector, circular septa were placed between all subdetector rings. In this way the scatter fraction could be limited to roughly 10–15%. Due to the limited energy resolution of BGO and in order to increase the sensitivity, a rather wide energy window was used. Currently systems can often be used both in 2D- and in 3D-mode or in 3D-only mode. Rather sophisticated software is available to correct for scattered radiation based on the individually measured transmission scan. Scatter correction in 3D is essential because the scatter

fraction can increase to 50% or even more depending on the part of the body which is imaged. Especially in 3D-mode, radiation can enter the block detector from a large opening angle. This introduces a kind of parallax which affects the spatial resolution in a negative way.

The gamma-spectrum from a patient is quite different from the spectrum from a point source in air because a lot of scatter will occur inside the body. In fact, most gamma quants will be scattered and will not be in the photo peak. The attenuation is described by: $I = I_0 \exp(-\mu x)$.

By using an external positron source, the individual attenuation can be measured. From a blank scan and a transmission scan, an attenuation map can be calculated. Because of the coincidence measurement, the position of the source in the body is not relevant, only the total thickness, d .

$$I = I_0 \exp(-\mu \cdot a) \cdot \exp(-\mu \cdot b) = I_0 \exp\{-\mu(a + b)\} = I_0 \exp(-\mu \cdot d)$$

Because of the coincidence measurement, the measured attenuation is independent of the position of the source, it can be performed by external sources [9, 10]. These sources are built into the gantry of the scanner. Normally a $^{68}\text{Ge}/^{68}\text{Ga}$ positron source, half-life 270 d/68 m, is used but experiments with singles sources (^{137}Cs) or CT images for attenuation correction have been implemented. With attenuation correction and scatter correction [11] calculated from individual attenuation measurements, a PET scanner is able to produce quantitative images in the sense that the activity per pixel can be measured in absolute terms (Bq/pixel). This is a unique feature of PET due to the use of coincidence measurements. To translate the CT images into a 511 keV attenuation map the CT images are segmented into the different tissues e.g. bone structures. The mass attenuation coefficients at 70 keV, the average energy in the CT spectrum, and at 511 keV are quite different, see Table 4.

Table 4: Mass attenuation coefficients μ/ρ (cm^2/g) for air, water, muscle and bone ^{*)}

	Air	H₂O	Muscle	Bone
70 keV	0.178	0.195	0.194	0.242
500 keV	0.0870	0.0968	0.0960	0.0927

^{*)} Radiological Health Handbook, revised edition, January 1970, U.S. Department of Health, Education and Welfare, Rockville, MD 20852, USA.

The counts acquired in a PET scan can be subdivided into the true coincidences, the scattered coincidences, and the accidental or random coincidences [13]:

$$N = N_{\text{true}} + N_{\text{scatter}} + N_{\text{acc}}$$

Scattered radiation is always present in the energy window set on the BGO detector due to the limited energy resolution of the detector and especially in 3D mode when the solid angle subtended by the individual detector block is increased by a large factor. Currently techniques are available for an individual scatter correction based on the measured attenuation. Accidental coincidences are possible due to the use of a finite time window:

$$N_{\text{acc}} = \Delta t \cdot N_{s1} \cdot N_{s2}$$

with Δt time window and N_{si} the single count rate in detector i .

By increasing the activity sufficiently the accidental count rate can always reach an area where it is the most prominent count rate.

For a more objective number on the count rate performance the Noise Equivalent Count rate (NEC_{rate}) has been introduced:

$$NEC_{rate} = T^2 / \{T + 2f_{obj} N_{acc} + S\},$$

with T the true coincident count rate, S the scattered count rate, N_{acc} the accidental count rate and f_{obj} the fraction of the field of view subtended by the object. This is a more objective figure for establishing the count rate performance of a PET scanner but one should agree on the size of the phantom to be used since this will determine f_{obj} and the scatter fraction. Since most patients are larger in diameter than most phantoms the NEC_{rate} curve for a patient will show a lower maximum which will be reached at a lower concentration of activity.

The spatial resolution achievable on a standard scanner now is roughly 4–5 mm FWHM and determined by the size of the detector in the block detector structure. Research is going on to achieve better spatial resolution by using smaller crystals and correcting for parallax by adding information on the depth of interaction (DOI) inside the crystal. A spatial resolution of ~ 2 mm FWHM can be achieved.

Limitations in spatial resolution for PET scanners can be divided into a fundamental and a technical limitation. The fundamental limitation is the finite range of the emitted positron. The maximum energy of the positron emitted is typical for each radioisotope. Since the surplus in energy has to be divided between the positron and the neutrino there is a continuous energy spectrum for the positron up to the maximum energy. The mean energy of the positron is roughly 40% of the maximum energy. So there is always a finite and unknown distance between the place of decay and place of annihilation. For a radionuclide like ^{18}F , with a very low maximum energy of 0.635 MeV, the maximum positron range in tissue (water) is 2.3 mm. The mean range in water is 0.6 mm. Nearly all other positron emitting radionuclides have a larger maximum energy, see Table 5. Another limitation is the deviation from 180° of the two annihilation quanta. From angular correlation experiments a finite width of 0.5° around the mean angle of 180° was established. Especially in scanners with a large radius this effect will become measurable.

Table 5: Positron energies, maximum and mean, and the respective ranges

Nuclide	$E_{\beta\text{max}}$ (MeV)	Range (mm)	$E_{\beta\text{mean}}$ (MeV)	Range (mm)
^{11}C	0.961	3.9	0.38	1.1
^{13}N	1.190	5.1	0.48	1.5
^{15}O	1.723	8.0	0.69	2.5
^{18}F	0.635	2.3	0.25	0.6
^{52}Fe	0.804	3.1	0.32	0.9
^{68}Ga	1.899	8.9	0.76	2.9
^{75}Br	1.740	8.1	0.70	2.6
^{82}Rb	3.350	17	1.34	5.9

The other limitation is the change from measuring line-integral projection into measuring the place of annihilation directly by means of a time of flight (TOF) measurement. As stated before, time differences of 3 ps have to be measured to obtain a spatial resolution of 1 mm. Detectors with these timing properties and also a high sensitivity for 511 keV gamma radiation are not known (yet). Recent experiments with LSO and LaBr_3 showed time resolution of 500 and 310 ps, respectively [14, 15].

4 Possibilities of PET in research and patient care

The clinical applications of PET are in the fields of cardiology, neurology, and oncology. The most frequently used radiopharmaceutical is ^{18}F FDG (^{18}F -2-fluoro-2-deoxy-D-glucose) which is a glucose analogue enabling the measurement of the glucose consumption *in vivo*. In cardiology, the

measurement of the myocardial blood flow under rest and stress conditions with ^{13}N -ammonia and the energy consumption with ^{18}F FDG is a standard examination to discriminate between ischemic and infarcted tissue. In neurology, measurement of cerebral blood flow and/or energy consumption of the brain is the standard examination. In oncology, PET is used for the detection of tumors and metastases and to measure the effect of therapy on tumor metabolism.

4.1 Applications in cardiology

Radiopharmaceuticals for cardiac studies are listed in Table 6. ^{13}N -ammonia is used for measurement of the myocardial bloodflow [16]. To study the viability, or glucose consumption, of the heart it is used in combination with ^{18}F FDG. The combination of an ammonia rest, an ammonia stress, and a metabolism study deliver a much too large number of images to evaluate individually. For this reason software to re-orient the images perpendicular to the long axis of the heart (left ventricle in fact) followed by a translation of the data into quantitative parameters of bloodflow and glucose consumption per heart region has been developed [17]. Bloodflow and metabolism are then presented for examination in a so-called polar map, see Figs. 5(a) and 5(b). It is also possible to use the electrocardiography to create a gated cardiac study. By cutting the cardiac cycle into small time-intervals and adding the data to these intervals, an image of the total cardiac cycle in time is created by this gated study. From these images of the beating heart the wall of the left ventricle can be detected, wall motion can be quantified [16, 17].

Table 6: Radiopharmaceuticals commonly used in cardiology

Measurement	Radiopharmaceutical
Blood flow	H_2^{15}O , $^{13}\text{NH}_3$, ^{82}Rb
Metabolism	^{18}F FDG, ^{11}C -fatty acids, ^{11}C -acetate
Receptor density	^{11}C -CGP
Hypoxia	^{18}F -fluoromisonidazol
Sympathetic function	^{11}C -meta-hydroxyephedrine (mHED)

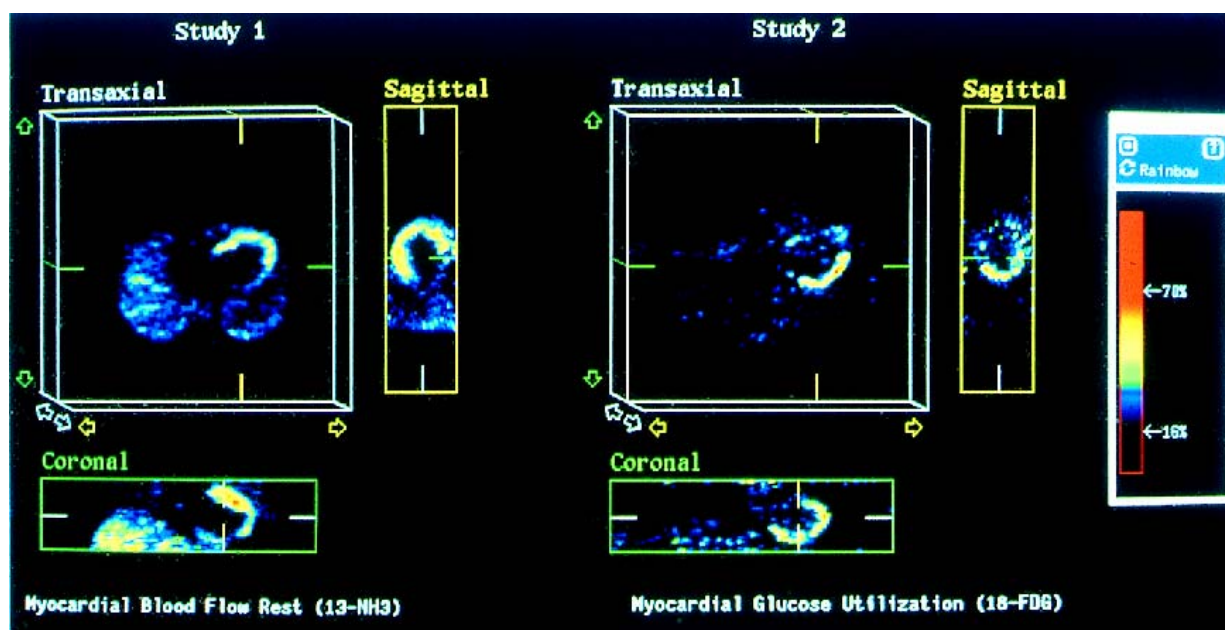


Fig. 5(a): Cardiac blood flow at rest (left) and glucose consumption (right) in one plane. Low flow and high glucose uptake is already visible and is quantitated in the data analysis, see Fig. 5(b).

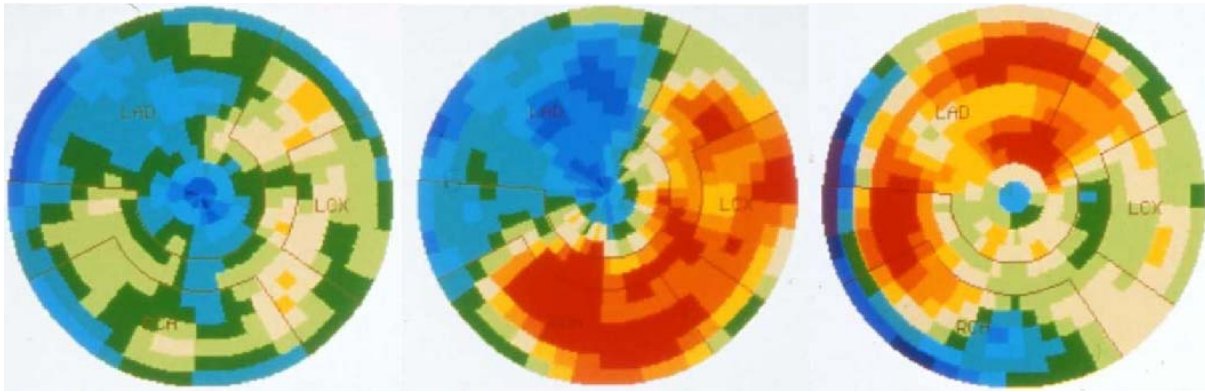


Fig. 5(b): Cardiac blood flow and glucose consumption as parametric polar map. Blood flow and glucose consumption were calculated per segment in the left ventricle after a dynamic data acquisition. Centre in each image is the apex of the heart. Left flow during rest, in the middle flow during exercise and at the right the glucose consumption. In the low-flow area a high glucose consumption is present signalling viable cardiac tissue. Bypass surgery will result in a normally functioning heart.

4.2 Applications in neuroscience

In Table 7, commonly used radiopharmaceuticals for neuroscience studies are listed. The clinical and research programmes in Groningen are focused on glucose metabolism (^{18}F FDG), bloodflow with H_2^{15}O , receptor studies, and gene therapy. For neuro-oncological studies, both ^{18}F FDG as well as ^{11}C -methionine are available. Software for the translation of measured radioactivity of ^{18}F FDG into glucose-consumption [18–21] has been developed. The dopamine transporter and the D_2 receptor in the human brain have been studied with ^{18}F -DOPA and ^{11}C -raclopride for quite some time [22, 23] especially in the case of Parkinson’s disease. Measurement of regional cerebral bloodflow (rCBF) with H_2^{15}O is of great importance to discover the functional anatomy of the brain in disciplines like cognitive neuroscience, linguistics, geriatrics (selective attention), and pharmacology (to measure the effect of drugs on the rCBF in different categories of patients). Stimulus research brings together nearly all disciplines: from biophysics through psychiatry to language [24–26]. Also the merging of functional PET images with anatomical MRI images, using segmentation techniques, is important to localize the functional anatomy. For analysis of rCBF studies, an important software package named Statistical Parametric Mapping (SPM) has been developed at the Functional Imaging Laboratory (FIL) in London [25] including the statistical inference of the generated data.

Table 7: Radiopharmaceuticals commonly used in neuroscience

Measurements	Radiopharmaceutical
Blood flow (rCBF)	H_2^{15}O , C^{15}O_2
Blood volume	^{11}C CO, C^{15}O
Oxygen extraction	Combination of above
Glucose metabolism	^{18}F FDG
Tumor metabolism	^{18}F FDG, ^{11}C -amino acids
Receptor measurements	^{11}C -methylspiperon, ^{18}F FESP, ^{18}F -DOPA, ^{11}C -raclopride
Stimulus research	^{18}F FDG, H_2^{15}O

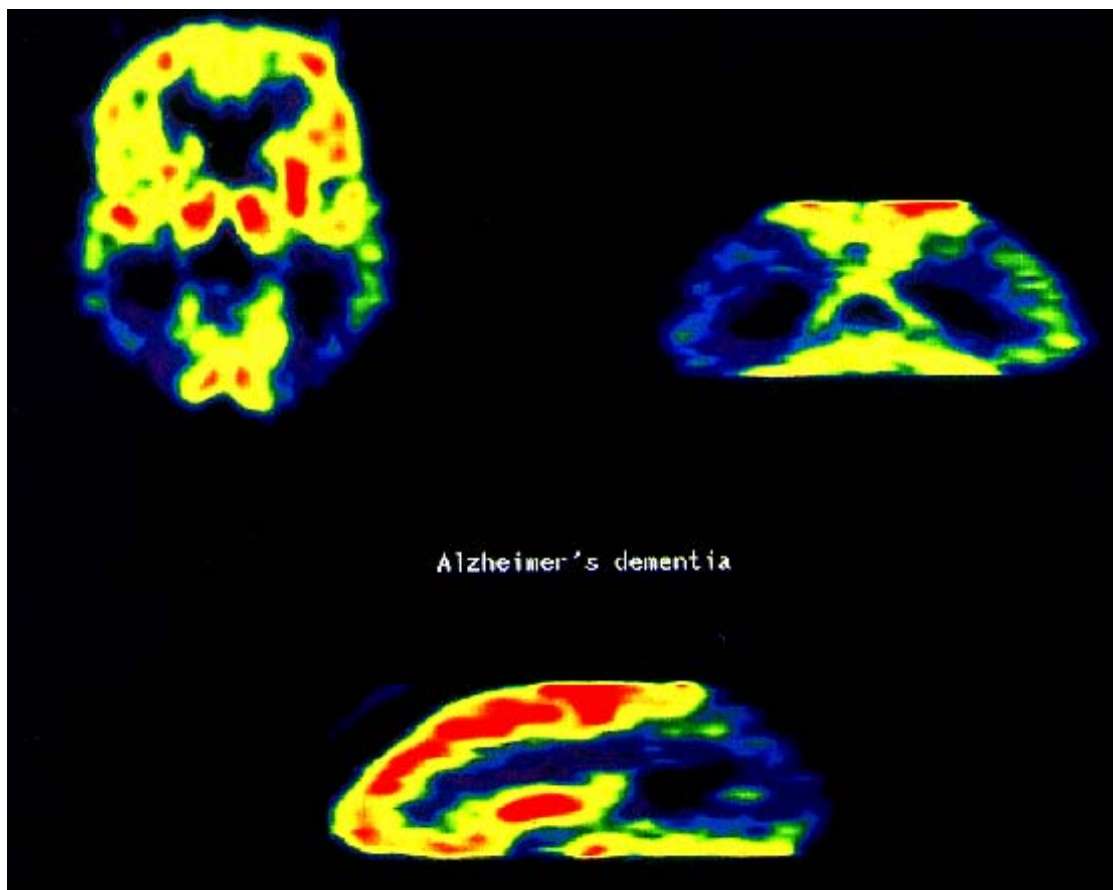


Fig. 6: Glucose consumption in the brain of patient with Alzheimer's disease. Glucose consumption in the occipital part of the brain is decreased by 50%.

4.3 Applications in oncology

In Table 8 different radiopharmaceuticals for oncological studies are summarized. For the study of tumor metabolism, ^{18}F FDG is most frequently used but other possibilities in the form of amino acids do exist. Also the effect of therapy on the tumor metabolism can be quantified by measuring before and after therapy. By performing the second study during the therapy a prognostic statement may also be possible. For brain studies the use of an amino acid can be favourable due to the better signal-to-noise ratio which can be obtained as compared to the glucose metabolism study. It is also possible to generate 'whole-body' images by projecting a number of consecutive transverse images into planar whole-body images [27]. In oncology, whole-body studies with ^{18}F FDG become the most frequently used mode of imaging, see Fig. 7. Moreover, ^{18}F FDG itself is (becoming) the most frequently used clinical application of PET in oncology which is also due to the fact that a number of studies have shown that this application of PET is cost effective and patient friendly [28–30]. In fact, due to the fact that ^{18}F FDG can be transported over distances of roughly 2 hours, many stand-alone PET scanners are being installed which are served from regional ^{18}F FDG 'factories'. Also the combination of PET and CT [31] into one device is of importance for matching functional and anatomical images in radiotherapy and surgery. The merging/matching of images of the human body below the brain is often very difficult or impossible because of repositioning problems of tissue on different scanners, by combining the scanners into one device this problem is avoided. The combined PET/CT scanners do have their impact on patient management for surgical and radiotherapy planning as well as on the assessment of tumor response [32, 33].

Table 8: Radiopharmaceuticals commonly used in oncology

Measurement	Radiopharmaceutical
Tumor perfusion	$H_2^{15}O$, $^{13}NH_3$
Tumor metabolism	^{18}F FDG, ^{11}C -tyrosine, ^{11}C -methionine, ^{11}C -choline, ^{11}C -thymidine, ^{18}F FLT
Cytostatica kinetics	^{11}C -cytostatics
Therapy evaluation	All of above by measuring before and after therapy

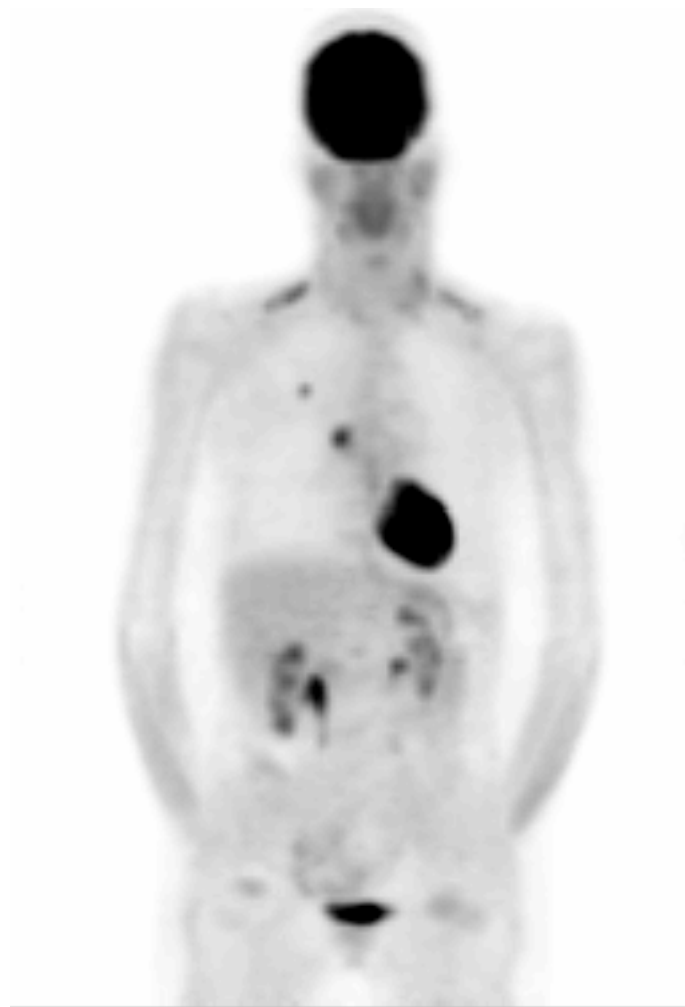


Fig. 7: Whole-body FDG scan. The high uptake in brain, heart and bladder is normal. Uptake in the lung shows two metastases.

4.4 Applications outside medicine

The labelling of new pharmaceuticals to establish their distribution *in vivo* is a technique by which the pharmaceutical industry can get information about possible efficacy of new drugs before large clinical studies are started. Large investments can be avoided in case of a negative finding or better rationalized in case of a positive finding.

The effect of new pharmaceuticals can be determined by measurement of differences in blood flow/glucose consumption/protein synthesis rate etc. before and after therapy. Dose effect relationships can also be studied.

In chemical reactors the exact localization of processes is sometimes completely unknown. Using nuclear techniques and especially PET it is possible, by scaling down reactor structures to fit the bore of a PET scanner, to obtain information which can be used to optimize the reactor [34].

5 Data analysis

A wide variety of data analyses is possible depending on the data acquisition protocol. One should understand that there are only a few measurable quantities on which the data analysis, often leading to functional parameters, can be based. In this part only some general remarks on data analysis will be made. In fact, each radiopharmaceutical has its own procedure for quantitative data analysis.

The PET scanner can deliver quantitative images (Bq/voxel) after correction for attenuation and scatter. The most simple analysis is an evaluation by visual inspection. Also ratios can be calculated by drawing ROI's (Regions Of Interest) in the images. Ratios of e.g. striatum/cerebellum, left/right can be calculated. Also the content or better the concentration of radioactivity within the ROI (Bq/ml) can be compared to the injected dose (Bq/g). The ratio of these two parameters is the Differential Absorption Ratio (DAR) or Standard Uptake Value (SUV). A DAR or SUV value of 1 indicates a homogeneous distribution. If something more elaborate, e.g., a functional parameter like blood flow (ml/min/100g), glucose consumption ($\mu\text{mol}/\text{min}/100\text{g}$) is required, a more complex analysis scheme has to be set up.

The problem is that there are very few measurable quantities on which a complex analysis can be based:

- Radioactivity (after all corrections) in tissue (Bq/voxel). The chemical identity is known only at the moment of injection, due to metabolism different metabolic species can be formed in course of time. Information on the radioactivity in tissue is available per voxel, per unit of time or per time frame.
- One can take (arterial) samples and measure the relative amounts of the different radioactive species in plasma as a function of time. The function describing the concentration of the original compound as a function of time is also known as the 'input function'. The PET scanner should be 'cross calibrated' with the well counter in which plasma or tissue samples are measured. The short half-life makes rapid chemical analyses necessary.

In any biological system we have to deal with a steady-state system which can be interpreted as a compartmental system [35]. Regardless of the fact that we have a continuous flow of materials, or of energy, the concentrations (or the chemical states) in the different compartments do not vary. The concentrations remain constant even though there is a flow of material along the chain. Positron emitting radiopharmaceuticals are normally compounds with a high specific activity. If the radiopharmaceutical is chemically identical to endogenous substances or is in competition with endogenous substances, we have to deal with compartment systems with distribution volumes and constant transfer flows. With X^* the amount of radioactive material is represented and with X the amount of non-radioactive material.

$$X^* + X = X, \quad \text{specific activity} = X^*/\{X^* + X\} = X^*/X.$$

A carrier-free production means that when producing X^* no X is formed. A non-carrier-added (nca) synthesis means that during the synthesis of X^* no carrier X is added, but some carrier is possibly included from the environment, e.g., atmospheric CO_2 .

In practice, as said before, only a limited number of quantities can be measured, and the number of free parameters and so the number of compartments has to be kept low in order to obtain a unique solution of the set of equations. Often compartment models are developed based on the metabolic pathway of a specific radiopharmaceutical and sometimes also non-linear terms are introduced, e.g., for ligand–receptor interaction. Also for receptor ligands specific compartment models have been introduced and by introducing reference tissues one tries to avoid (arterial) blood samples [36].

This is possible, for example, in brain receptor studies in those cases where it is known that in certain areas of the brain no receptors of interest are present as is the case for the dopamine receptor in the cerebellum. A detailed analysis of the possibilities in two and three compartment systems is given by Willemsen and van den Hoff [37]. Figure 5(b), showing blood flow (rest and stress) and glucose consumption in the left ventricle is in fact the result of such a compartment model analysis.

Another frequently used technique in neurological research is the measurement of the regional cerebral blood flow (rCBF). These measurements are often used in cognitive neuroscience experiments or in language studies in which two conditions are created which are measured a number of times and the results are then subtracted in order to find those areas in the brain which show increased blood flow in response to a stimulus. Analysis of a repeated study in one person or in multiple persons including realignment and normalization of the brain based on the measured rCBF followed by a statistical inference can be obtained, e.g., in the SPM package as developed by the FIL in London [25].

6 Dosimetry

The International Committee on Radiological Protection (ICRP) gives international recommendations on radiation protection. The ICRP publications provide all relevant information. The radiation dose of a PET study can be calculated in conformity to the recipe as developed by the Medical Internal Radiation Dose (MIRD) Committee of the Society of Nuclear Medicine (SNM). The MIRD system handles the concept of source and target organs [38]. Each organ is a target for radiation from a radiopharmaceutical deposited in the body. An organ that contains radioactivity is not only a source but also a target due to self-irradiation. The radiation dose received by target organs depends on the geometry inside the body and the nature and energy of the radiation and of course the metabolic pathway of the employed radiopharmaceutical [39,40]. The radiation dose for each radiopharmaceutical can be established by measuring the radioactivity per organ as a function of time. From these measurements the integral of the activity curve for a source region per organ can be calculated and is used as input for the OLINDA/EXM computer code, the successor of the widely used MIRDOSE3.1 code, to calculate the radiation dose [41, 42]. Questions on the nature, types, and magnitudes of radiation risks together with the principles of research design involving the use of ionizing radiation are addressed in the ICRP 62 publication [43]. The radiation dose in most clinical PET studies is of the order of 5 mSv.

7 New developments

The cyclotron as available now for PET centres is different from the older machines used in the field of nuclear physics not only because of the limited number of particles and fixed energy but also because of the incorporation of the targetry for production of the most important radionuclides. Automation and computer control is integrated into the design. Not only the beam quality but also the beam current is a major parameter because the current determines the production capacity. Beam quality is not that crucial for radionuclide production and in fact the beam power density (W/cm^2) should not be too high in order to avoid burning holes in the target foils and the target itself. For the

day-to-day operation no separate operating team is required, the cyclotron can be operated by the technical/chemical staff because of the ease of operation of the present cyclotron control systems.

The developments over the last decade seem to have stabilized into cyclotrons, especially for the four most important PET radionuclides, at two different energy levels, but both with the acceleration of negative ions. These are cyclotrons with a proton beam around 12 MeV and those with a proton beam energy around 17 MeV. The first being smaller and the cheapest, the second having a higher production capacity because their thick target yield is higher by nature, but more expensive. Lower energy leads also to less penetrating particles and consequently to thinner targets with a lower yield. Consequently the target technology becomes more difficult and more critical by this reduction in beam energy because the beam current has to be increased to keep up in production capacity. If a more general radionuclide production unit is necessary, a cyclotron with a proton beam energy of around 30 MeV would be the cyclotron of choice.

Some cyclotron manufacturers also provide local movable shielding of concrete and lead or boronated water fitting rather tightly around the accelerator, resulting in lower total mass of the shielding.

The radiation detectors used in positron cameras at the moment are made of BGO, GSO or LSO; NaI has also been used but is obsolete for the present PET scanners. Although BGO has a high stopping power for 511 keV and a number of other favourable properties, the light yield of NaI is much higher. The ideal detector for a positron camera should have a time resolution of less than 10 ps and this combined with other properties like high stopping power, high Z , non-hygroscopic etc. This extremely fast timing would allow measurement of the place of annihilation within a few millimetres by means of the time-of-flight (TOF). With the present detectors only the line on which the annihilation took place is determined. The filtered back-projection reconstruction technique in combination with a block structure of the detectors makes a spatial resolution of 4–7 mm FWHM standard. The scintillator LSO combines the good properties of BGO with high light yield (75% of the yield of NaI) and is also rather fast (40 ns). A disadvantage is the presence of a natural radioactive isotope of lutetium but this will not influence the image formation in a PET scanner. The higher light yield will improve the energy resolution and therefore decrease the scatter fraction.

At the moment, PET scanners are being built for small animals (rats and mice) and a spatial resolution of less than 2 mm FWHM has been achieved in these systems [38]. High resolution studies in small animals are becoming more important because next to the pharmacokinetic information from normal animals for molecular imaging, animal models with human diseases are becoming available. Different detector materials are being used in these animal scanners: BGO, GSO, LSO, LYSO, LuYAP and Ar in a gas-filled MWPC (Multi Wire Proportional Counter). To increase the spatial resolution sometimes depth of interaction (DOI) is implemented by using two layers of detectors. By pulse-shape discrimination the layer of interaction is established and by this a better position definition.

In order to solve the matching problems between PET and CT images, combined PET/CT machines have been developed. In fact these are separate PET and CT tomographs put together in one cabinet operating independently but under one general software system so the images have the same pixel size etc. In this way the changes in positioning which always occur if a patient is transferred from one scanner to another are avoided. The advantages of combined functional and anatomical images are in the fields of head/neck surgery, pulmonary surgery and also in radiotherapy, especially when conformal therapy is considered [31, 32]. An additional advantage is the gain in time when the CT information is used for the attenuation correction. The transmission scan with an external source is roughly three minutes per bed position while the CT scan takes only seconds, so a substantial gain in throughput can be achieved in whole-body studies. Efficacy studies are becoming available for the evaluation of the clinical value of these combined machines.

8 PET and other imaging modalities

The most common imaging technique in medicine uses X-rays. In its most simple form a density projection is generated by holding the subject of interest between the X-ray tube and a photographic plate. The advanced form can be found in a CT scanner in which a rotating X-ray source and detectors make a transverse section image [45] in the form of a density map. Due to the large difference in density between bones and tissue the bones can be visualized perfectly while small differences in tissue density will be more difficult to visualize, see also Table 4. The use of contrast agents, like fluids with high densities and high-Z components, can change the differences in density and therefore the interpretation of the images dramatically.

The Nuclear Magnetic Resonance (NMR) technique is in use to visualize the protons (bound to water) in the human body. Homogeneous magnetic fields up to 3 T are in use in medical NMR scanners, nowadays abbreviated to MRI (Magnetic Resonance Imaging). In order to have a short imaging time, gradient fields with frequency decoding are used. The strength of the NMR signal is proportional to the difference in population of the spin-up and spin-down state. Under normal conditions at room temperature the ratio between spin-up and spin-down is rather close to unity [46]. The NMR technique is a rather insensitive technique for this reason but is successful because of the high water concentration in the human body. Also paramagnetic contrast agents like Gd-DTPA can be used to increase the contrast. Both the X-ray and the MRI technique supply anatomical information.

With NMR, information on the structure of molecules can also be obtained, as is done in chemistry. This is also possible in the human body but limited to the brain and to molecular structures which have a concentration of 0.1 mM or more as a rule of thumb. The limitation to mainly brain tissue is because the signals from water and fatty tissues (triglycerides) have to be suppressed and these concentrations are rather low in the brain in contrast to the thorax, for example.

Functional MRI, or fMRI, uses the effect of deoxyhemoglobin on the MRI signal, the so-called blood-oxygen-level-dependent (BOLD) signal change [47]. This signal is interpreted as changes in rCBF and is used for stimulus experiments. fMRI and PET are therefore sometimes considered as competitive approaches. However, the mechanisms underlying the BOLD signal change are not yet fully understood. The quality of fMRI as a research tool can be judged by the results of the experimental applications and also by a cross-validation with the gold standard for the brain: $H_2^{15}O$ PET measurements for measuring the rCBF. Since the sensitivity, spatial resolution, temporal resolution, etc. of both techniques are quite different, a complementary approach will probably yield the best results. In case noise is a problem or movement artefacts are easily achieved; in case of metallic implants PET has to be preferred. Each experiment should be evaluated for the most promising experimental technique.

By using radionuclides bound to different molecular structures functional emission imaging became available in the 1950s. It is functional imaging because chemical structure and human metabolism determine the fate of the molecule *in vivo*, with PET as the ultimate form of nuclear medicine. The high specific activity (TBq/ μ g) achievable, inherently linked to the production method, is of importance, for example, for receptor research and makes it possible to perform 'tracer' experiments.

Since the PET method supplies functional information, the combination with X-ray and NMR techniques, CT and MRI, yields information on the functional anatomy. In order to make this combination, the images of the different disciplines should be available in a transparent way and image resize and re-orientation techniques should be available to match the images from the different modalities. In some institutions, the comparison and transformation of PET images to a stereotactic brain atlas have also been performed. The head and brain are the structure/organ of choice to evaluate 'multi-modality' matching for obvious reasons. Below the brain it is more difficult due to differences in positioning inside the scanner. For that reason, the first commercial PET/CT machines are entering

the market and their possibilities will be evaluated in the near future. Matching software with non-linear components is becoming available in order to match PET, CT, and MRI images in the thorax and abdominal regions.

References:

- [1] Friedlander G, Kennedy JW, Macias ES, Miller JM, Nuclear Radiochemistry, 3rd Edition, John Wiley & Sons, 1981.
- [2] Radionuclides Production Vol I & II, ed. F. Helus, CRC Press, 1983, ISBN 0-8493-6003-X & 0-8493-6004-8.
- [3] Stocklin G and Pike VW (eds), Radiopharmaceuticals for Positron Emission Tomography, Kluwer Academic Publishers, 1993, ISBN 0-7923-2340-8.
- [4] Enge HA, Introduction to Nuclear Physics, Addison-Wesley Publishing Company, 1969.
- [5] Sorensen JA and Phelps ME, Physics in Nuclear Medicine, 2nd edition, Saunders, 1987; Cherry S, Sorensen JA, Phelps ME, Physics in Nuclear Medicine, 3rd Edition, Harcourt Health Sciences, ISBN 072168341X, Nov. 2001.
- [6] Cho ZH, Jones JP and Singh M, Foundations of Medical Imaging, John Wiley & Sons, 1993
- [7] Herman GT (ed), Image Reconstruction from Projection, Topics in Applied Physics, vol. 32, Springer, 1979.
- [8] Phelps ME, Cherry SR, The changing design of positron imaging systems, Clin. Pos. Imaging **1** (1998) 31–46.
- [9] Phelps ME, Proc. Natl. Acad. Sci. USA **97** (2000) 9226–9233.
- [10] Hoffman EJ Huang SC, Phelps ME, Quantitation in Positron Emission Computed Tomography: 1. Effect of size of object, JCAT **3** (1979) 299–308.
- [11] Huang SC, Hoffman EJ, Phelps ME, Kuhl DE, Quantitation in Positron Emission Computed Tomography 2: Effects of inaccurate attenuation correction, JCAT **3** (1979) 804–814.
- [12] Watson CC, Newport D, Casey ME, deKemp RA, Beanlands RC and Schmand M, IEEE Trans. Nucl. Sci. **44** (1997) 90–97.
- [13] Hoffman EJ, Huang SC, Phelps ME, Kuhl DE, Quantitation in Positron Emission Computed Tomography 4: Effect of accidental coincidences, JCAT **5** (1981) 391–400.
- [14] Doorenbos P, de Haas JTM and van Eijk CWE, Gamma ray spectroscopy with a 19x19 mm³ LaBr₃ : 0.5% Ce³⁺ Scintillator, IEEE Trans. **NS51** (2004) 1289–1296.
- [15] Kuhn A, Surti S, Karp JS, Raby PS, Shah KS, Perkins AE and Muehlelehner G, Design of a lanthanum bromide detector for time-of-flight PET, IEEE Trans. **NS51** (2004) 2550–2557.
- [16] Porenta G, Czernin J and Schelbert HR, in Positron Emission Tomography of the Heart, Bergmann SR and Sobel BE (eds), Futura Publishing Company, Inc., 1992, 153–183.
- [17] Willemsen ATM, Blanksma PK, Paans AMJ, in Cardiac Positron Emission Tomography: viability, perfusion, receptors and cardiomyopathy, van der Wall EE, Blanksma PK, Niemeyer MG and Paans AMJ (eds), Kluwer Academic Publishers, 1995, 87–96.
- [18] Sokoloff L, Reivich M, Kennedy C, Des Rosiers MH, Patlak CS, Pettigrew KD, Sakurada O and Shinohara M, J. Neurochem. **28** (1977) 897–916.
- [19] Phelps ME, Huang SC, Hoffman EJ, Selin C, Sokoloff L and Kuhl DE, Ann. Neurol. **6** (1979) 371–388.

- [20] Wienhard K, Measurement of glucose consumption with [¹⁸F]-Fluorodeoxyglucose, *Methods* **27** (2002) 218–215.
- [21] Herholz K, Herscovitch, Heiss W-D, *NeuroPET, PET in Neuroscience and Clinical Neurology*, Springer Verlag, ISBN 3-540-00691-5, 2004.
- [22] Baron JC, Comar D, Farde L, Martinot JL, Mazoyer B (eds), in *Brain Dopaminergic Systems: Imaging with Positron Tomography*, Kluwer Academic Publishers, 1991.
- [23] Van Waarde A, Vaalburg W, Doze P, Bosker FJ, Elsinga PH, PET imaging of Beta-Adrenoceptor in the human brain: A realistic goal or a mirage?, *Curr. Pharm. Des.* **10** (2004) 1519–1536.
- [24] Toga AW and Mazziotta JC (Eds), *Brain Mapping; The Methods*, Academic Press, 1996.
- [25] Frackowiak RSJ, Friston KJ, Frith CD, Dolan RJ, Mazziotta JC (eds), *Human Brain Function*, Academic Press, 1997.
- [26] Aine CJ, *Crit. Rev. Neurobiol.* **9** (1995) 229–309.
- [27] Budinger TF, Brennan KM, Moses WW and Derenzo S, *Nucl. Med. Biol.* **23** (1996) 659–667.
- [28] Conti PS, Lilien DL, Hawley K, Keppler J, Grafton S and Bading JR, *Nucl. Med. Biol.* **23** (1996) 717–735.
- [29] Valk PE, Pounds TR, Tesar RD, Hopkins DM, Haseman MK, *Nucl. Med. Biol.* **23** (1996) 737–743.
- [30] Pieterman RM, van Putten JWG, Meuzelaar JJ, Mooyaart EL, Vaalburg W, Koeter GH, Fidler V, Pruijm J and Groen HJM, *New Eng. J. Med.* **343** (2000) 254–261.
- [31] Beyer T, Townsend DW, Brun T, Kinahan PE, Charron M, Roddy R, Jerin J, Young J, Byars L, Nutt R, *J. Nucl. Med.* **41** (2000) 1364–1374.
- [32] Klutz PG, Meltzer CC, Villemagne VL, Kinahan PE, Chander S, Martinelli MA, Townsend DW, *Clin. Pos. Imag.* **3** (2000) 223–230.
- [33] Valk PE, Bailey DL, Townsend DW, Maisey MN, *Positron Emission Tomography, Basic Science and Clinical Practise*, Springer Verlag, 2002, ISBN 1852334851.
- [34] Dechsiri C, Ghione A, van denWiel F, Dehling HG, Paans AMJ, Hoffmann AC, *Positron emission tomography applied to fluidization engineering*, *Can. J. Chem. Eng.* **83** (2005) 88–96.
- [35] Rescigno A, Segre G, *Drug and Tracer Kinetics*, Blaisdell Publishing Company, Waltham (Mass), 1966.
- [36] Lammertsma AA, Hume SP, *Neuroimage* **4** (1996) 153–158.
- [37] Willemsen ATM, van den Hoff J, *Current. Pharm. Des.* **8** (2002) in press.
- [38] *MIRD Primer*, Loevinger R, Budinger TF, Watson EE, SNM, 1991.
- [39] *Radiation dose to patients from radiopharmaceuticals*, ICRP Publication 53, Pergamon Press, 1987.
- [40] *Radiation dose to patients from radiopharmaceuticals*, ICRP Publication 80, Pergamon Press, 1999.
- [41] Jansen HML, Knollemans S, Veenma L, Willemsen ATM, Wiersma A, Franssen EJJ, Russel FGM, Korf J and Paans AMJ, *Pharmacokinetics and dosimetry of cobalt-55 and cobalt-57*, *J. Nucl. Med.* **37** (1996) 2082–2086.
- [42] Stabin MG, Sparks PB, Crowe E, *OLINDA/EXM: The second-generation personal computer software for internal dose assessment in nuclear medicine*, *J. Nucl. Med.* **46** (2005) 1023–1027.

- [43] Radiological Protection in Biomedical Research, ICRP Publication 62, Pergamon Press, 1992.
- [44] Chatziioannou AF, *Eur. J. Nucl. Med.* **29** (2002) 98–114.
- [45] Barrett HH and Swindell W, *Radiological Imaging*, Academic Press, 1981.
- [46] Gadian DG, *Nuclear Magnetic Resonance and Its Applications to Living Systems*, Clarendon Press, Oxford (UK), 1982.
- [47] Moonen CTW and Bandettini PA (Eds), *Functional MRI*, Springer Verlag, 2000.